Mechanical and physical properties of ultra-oriented polyoxymethylene produced by microwave heating drawing

T. Konaka, K. Nakagawa and S. Yamakawa
Ibaraki Electrical Communication Laboratory, Nippon Telegraph and Telephone Public Corporation, Tokai, Ibaraki 319-11, Japan
(Received 10 January 1984; revised 8 June 1984)

The properties of ultra-oriented polyoxymethylene tubes produced by drawing under microwave heating have been assessed by mechanical testing, optical microscopy, scanning electron microscopy, X-ray analysis, birefringence and differential scanning calorimetry. The highest Young's modulus of 58 GPa was obtained at room temperature (77 GPa at −150°C) at a draw ratio of 33. The maximum tensile strength was 1.7 GPa at a draw ratio of 26. The nonuniformity of Young's modulus in a radial direction has been compared with the nonuniformity of the birefringence and heat of fusion.

(Keywords: polyoxymethylene; property; drawing; microwave heating)

INTRODUCTION

Recently, techniques for the production of ultra-high modulus oriented polymers have been investigated by many workers[1]. Polyoxymethylene (POM) is one of the most investigated polymers in the production of ultra-high modulus polymers. The POM crystal modulus has been estimated theoretically to be 95–153 GPa[2–4] and experimentally 53–189 GPa[5–9]. An ultra-oriented fibre, which has a Young's modulus of 35 GPa (draw ratio of 20), was produced by a two-stage drawing process[10]. Brew and Ward obtained a Young's modulus of 39.5 GPa by drawing a dumbbell shaped POM sample up to a draw ratio of 23 using a conventional tensile testing machine[11]. Oriented POM rods possessing Young's moduli up to 24 GPa were produced at relatively low production rates by hydrostatic extrusion[12] and die drawing[13]. We have already reported that ultra-high modulus POM rods, tubes and tapes can be produced by microwave heating drawing[8,14,15]. For example, tubes possessing Young's moduli up to 63 GPa were produced at draw ratios up to 30. This new drawing technique has enabled us to produce continuously thick section samples such as rods, tubes, tapes, etc.

In this paper the mechanical and physical properties have been examined for the ultra-oriented POM tubes produced by this drawing technique.

EXPERIMENTAL

Sample preparation

The tube with outer and inner diameters of 3 mm and 1 mm, respectively, was produced from a commercially available POM (Delrin 100, $\bar{M}_n = 66\,000$) by melt-extruding. The tube was drawn on a microwave heating drawing apparatus[14,15] at a feed speed of 0.06 m/min and a maximum ambient temperature of 135°C.

Mechanical measurements

The static tensile, dynamic and sonic moduli were measured. The tensile modulus was determined from the initial slope of the stress–strain curves at room temperature obtained by using a tensile testing machine. The sample gauge length was 150 mm and the crosshead speed was 5 mm/min. The strain was measured for the part of the specimen with distance marks of 50 mm using an extensometer. The cross-sectional areas of the tubes were determined from the weight per unit length and the densities were measured at 23°C in a density gradient column containing a mixture of toluene and carbon tetrachloride. The densities were in the range of 1.41–1.43 g cm^{-3}. The draw ratios were determined from these cross-sectional areas.

The dynamic modulus was measured at 3.5 Hz and at an amplitude of ±25 μm on samples 70 mm long using Rheovibron DDV-3-EA (Toyo Baldwin Co., Ltd., Japan).

The sonic modulus[16] was measured at room temperature using a direct reading pulse propagation visco-elastometer DDV-5-B (Toyo Baldwin Co., Ltd., Japan). The pulse frequency was 10 kHz and the pulse propagation length was 200 mm.

The tensile strength was measured at room temperature on a tensile testing machine using two Al reel chucks of 80 mm diameter. The distance between the centre of the reels was 100 mm and the crosshead speed was 100 mm min^{-1}. The tensile strength tests were followed using a video camera and recorder. On the video frames, the tensile elongation at break was determined from the change of the distance between two marks written on the sample.

Optical and scanning electron microscopy

The drawn tubes mounted into an epoxy resin were cut vertically to the drawing direction and their surfaces were polished. These cross-sections were examined under an

0032-3861/85/030462-07$03.00

optical microscope. The cross-section of the tubes, which were cleaved parallel to the drawing direction in liquid nitrogen, were examined under a scanning electron microscope.

X-ray measurements

Wide-angle X-ray diffraction was measured at room temperature with a diffractometer (Rigaku-Denki Co., Japan). The azimuthal profiles of the peaks were measured using a nickel-filtered 50 kV/150 mA CuKα radiation focussed by a 1 mm collimator. The receiving slit was 2° and the scanning speed was 4°/min. The crystalline orientation (f_c) was calculated from an azimuthal half-width of a (100) plane reflection[17], assuming a Gaussian curve[18]. X-ray photographs were taken with a Raue camera, using a 0.5 mm collimator.

Birefringence measurements

The drawn tubes were sliced parallel to the drawing direction to about 20 μm thickness with a microtome. Birefringence (Δn) was determined from the retardation (R) measured by a polarized microscope XTP-11 (Nicon Co., Japan) with a beam of 0.1 mm, using the following equation,

$$\Delta n = R/d \qquad (1)$$

where d is the sample thickness.

Differential scanning calorimetry

The melting behaviour of the drawn tubes was examined using a Perkin-Elmer DSC-2. A heating rate was 10°C/min and the sample weight was about 5.0 mg. The temperature and the heat of fusion were calibrated with indium.

RESULTS AND DISCUSSION

Mechanical properties

Figure 1 shows typical stress–strain cycles of a drawn POM tube (draw ratio of 33). The tube behaved elastically at the strain less than 0.4%. The cycles show hysteresis over this strain.

Figure 2 shows the draw ratio dependence of Young's moduli which were obtained by the static tensile test, dynamic mechanical measurement and sonic pulse propagation measurement. The Young's modulus increases with draw ratio and the highest value of 58 GPa was obtained at a draw ratio of 33. The tensile modulus is consistent with the dynamic modulus. But the sonic modulus becomes smaller than the others at draw ratios greater than about 20.

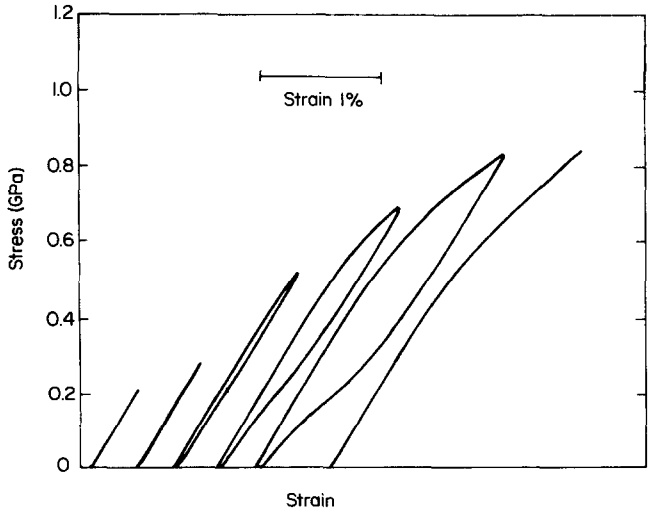

Figure 1 Stress–strain cycles of ultra-drawn POM tubes (draw ratio of 33) recorded at room temperature

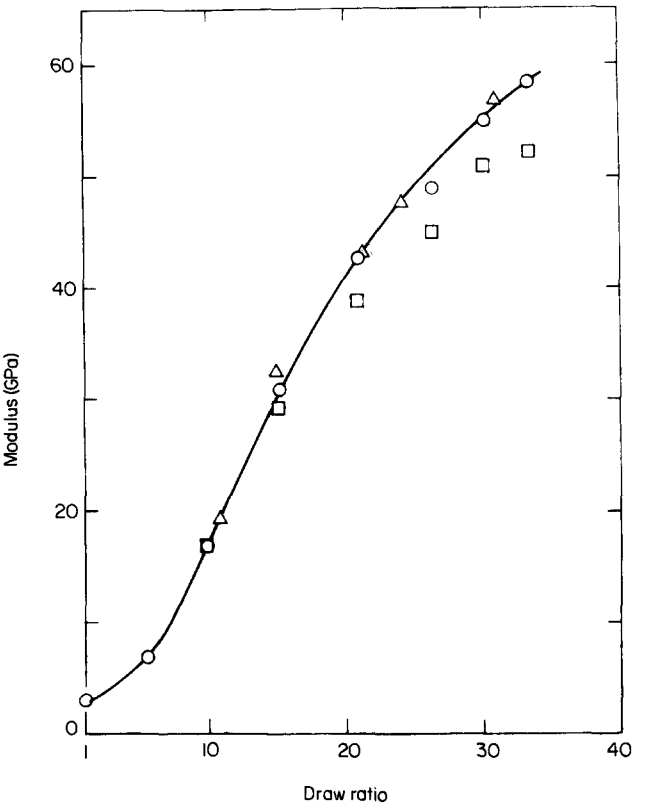

Figure 2 Young's modulus vs. draw ratio for POM tubes. (○) Tensile modulus, (△) dynamic modulus, (□) sonic modulus

Figure 3 shows the draw ratio dependence of tensile strength and elongation at break. The original POM tube has a tensile strength of 0.07 GPa. The tensile strength increases and passes through a maximum with the draw ratio. The maximum strength is 1.7 GPa at a draw ratio of 26. This maximum strength corresponds to that of the POM fibre produced by a two-state drawing process[10]. The tensile elongation at break decreases with draw ratio. For example, the elongation at break is about 8% and 3% at draw ratios of 10 and 33, respectively.

Figures 4 and *5* show the temperature dispersions of the dynamic modulus and tan δ (heating rate of 2°C/min), respectively. The most striking feature is that the very high modulus of 77 GPa at −150°C is achieved at the highest draw ratio. The value is comparable with the crystal modulus of 95–153 GPa obtained from theory[2-4] and experiment[6-8]. Both α and γ relaxations[19], which are associated with substantial changes of modulus and tan δ, are clearly visible. It can be seen from the Figures that all drawn samples show a plateau region with a span from −50°C to 100°C in which the modulus is less dependent of temperature and the loss tangent falls to nearly zero. The α relaxation peak moves to higher temperatures with increasing draw ratio, while the γ peak moves to lower temperatures. The intensities of both peaks decreases with draw ratio. The decrease in γ peak intensity shows that the local motions of molecular chains in the noncrystalline region and defect regions within the crystal are suppressed with draw ratio.

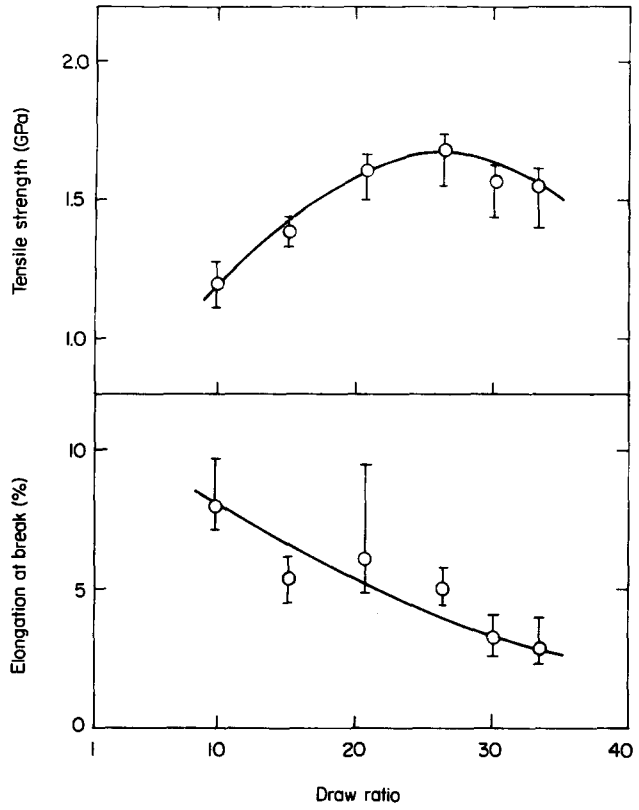

Figure 3 Tensile strength and elongation at break vs. draw ratio for POM tubes

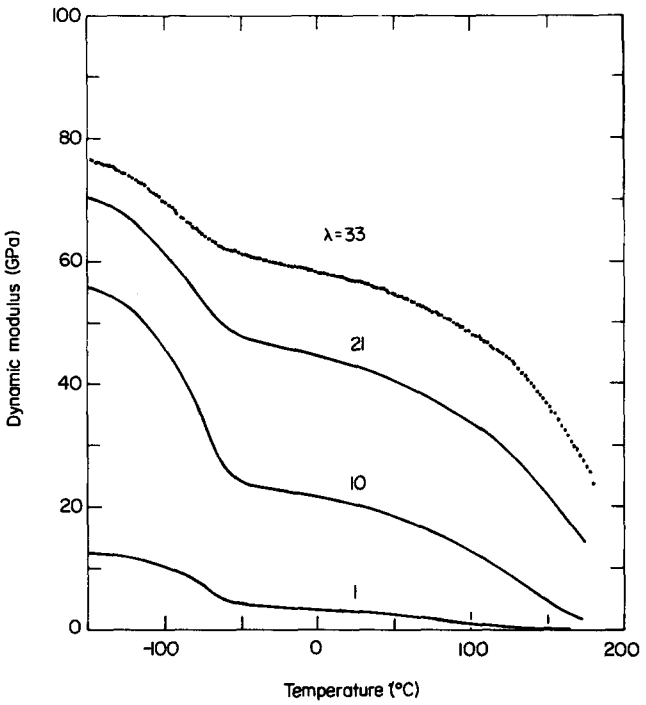

Figure 4 Dynamic modulus vs. temperature for POM tubes at different draw ratios

Void formation

The outer and inner diameters of the drawn tubes were measured from the photograph of the cross section. In *Figure 6* the diameters are compared with those calculated using a relation $D^2 = D_0^2/\lambda$ where D is the diameter at draw ratio (λ) and D_0 is the diameter before drawing ($\lambda = 1$). Both the inner and outer diameters were calculated using this equation. This equation corresponds to an ideal deformation mode in which the density is assumed to remain constant during drawing. In *Figure 6* the observed values follow calculated curves at draw ratios less than 20, suggesting the ideal mode of deformation. However, the deviations become appreciable above $\lambda = 20$, particularly in the outer diameter. This suggests the extensive formation of internal voids. The volume fraction of internal voids (f_v) was calculated using the formula[20]

$$f_v = 1 - \rho_{app}/\rho \qquad (2)$$

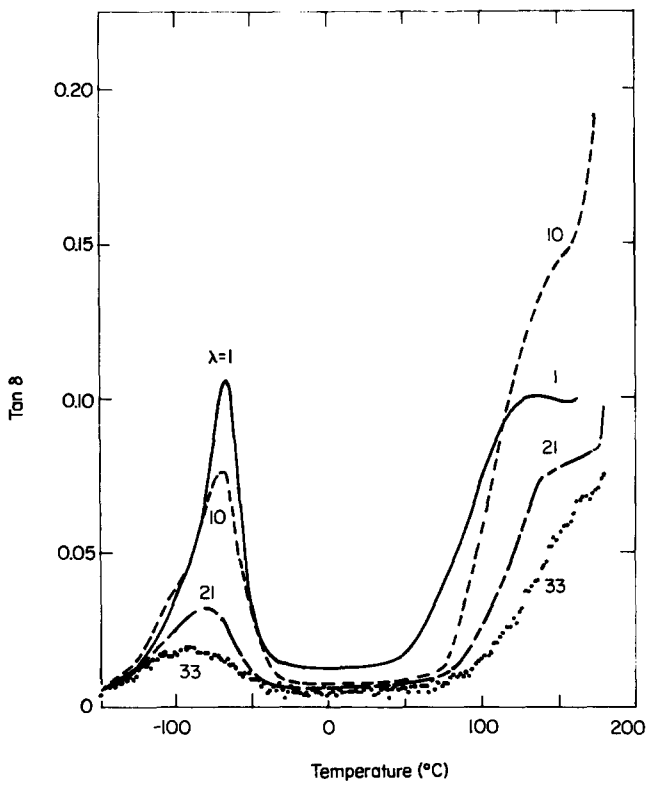

Figure 5 Tan δ vs. temperature for POM tubes at different draw ratios

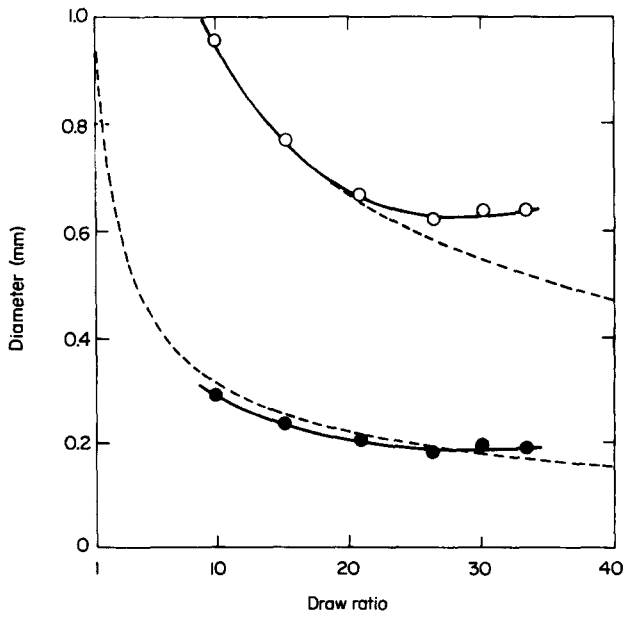

Figure 6 Diameter vs. draw ratio for POM tubes. (○) Outer diameter, (●) inner diameter, broken line:calculated diameter

where ρ_{app} denotes the apparent macroscopic density determined from the weight and dimension and ρ is the density measured by the gradient column method. The calculated void fraction is shown in *Figure 7*. The void fraction increases at draw ratios over about 20 and it reaches 0.33 at a draw ratio of 33. For example, the void fraction of about 0.28 is reported for a highly oriented polyethylene[20].

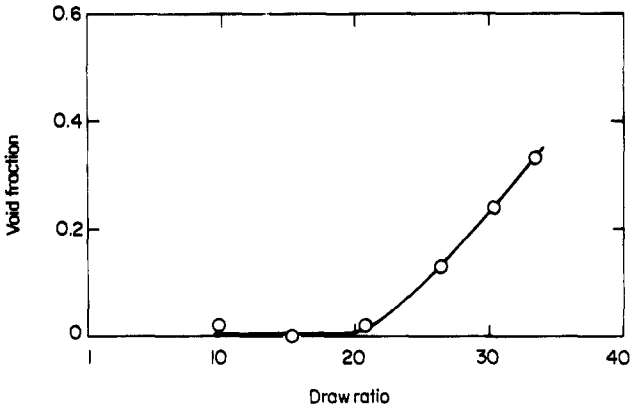

Figure 7 Void fraction vs. draw ratio for POM tubes

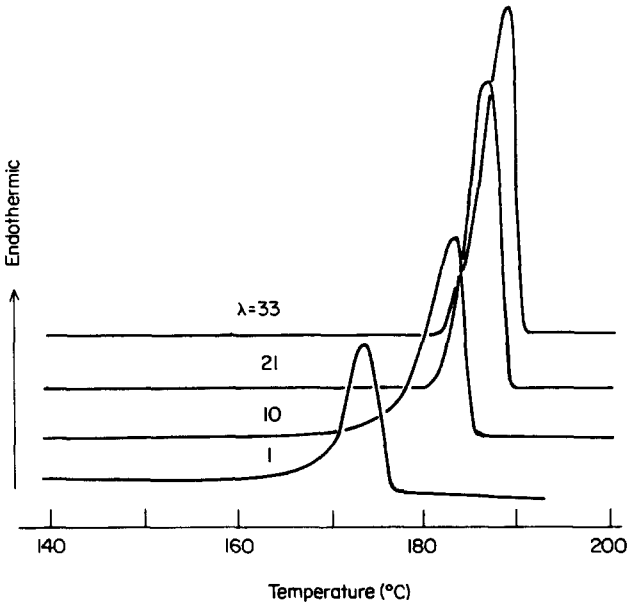

Figure 8 D.s.c. heating thermograms of POM tubes

Crystallinity

Figure 8 shows the d.s.c. heating thermograms of drawn POM tubes. The melting peak becomes sharp and moves to high temperatures with draw ratio. *Figure 9* shows the draw ratio dependence of the melting temperature, determined from the peak maximum, and the heat of fusion, indicating that they both increase with draw ratio. The highest values of melting temperature and heat of fusion are 189°C and 56.3 cal/g at a draw ratio of 33. This heat of fusion gives a crystallinity of about 75% based on a crystal heat of fusion of 75.3 cal/g[21].

Orientation

Figure 10 shows wide-angle X-ray diffraction patterns, indicating a very high degree of crystalline orientation. The crystalline orientation function is very close to unity at draw ratios over 10 as shown in *Figure 11*.

Figure 12 shows the average birefringence over the

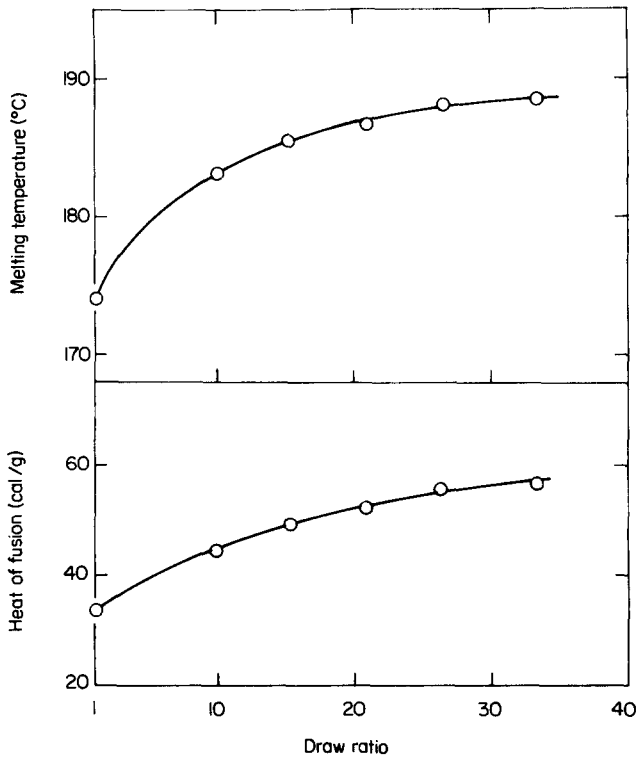

Figure 9 Melting temperature and heat of fusion vs. draw ratio for POM tubes

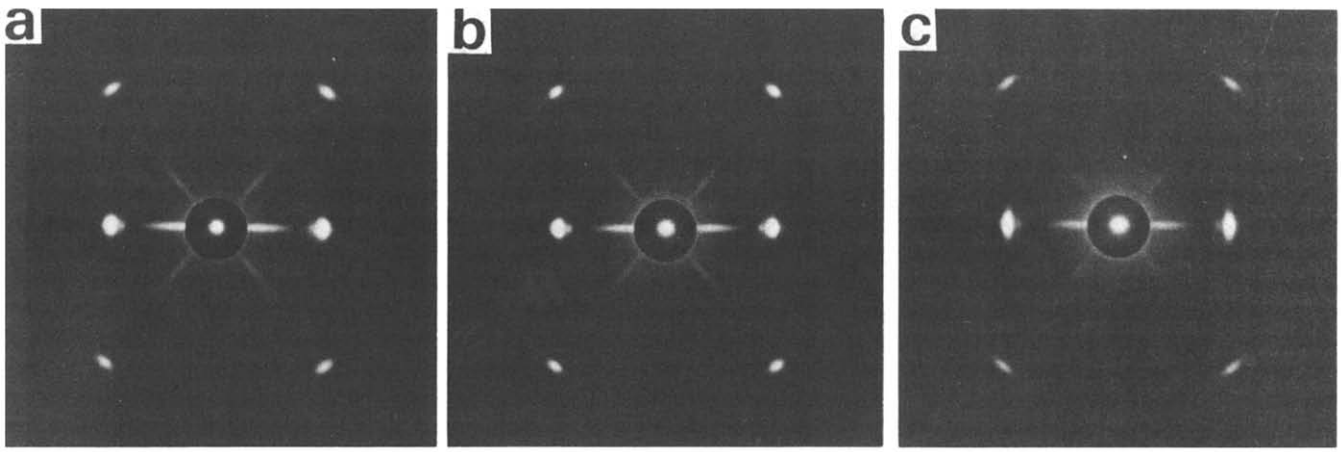

Figure 10 Wide-angle X-ray diffraction patterns of POM tubes, draw ratios: (a) 10, (b) 21, (c) 33

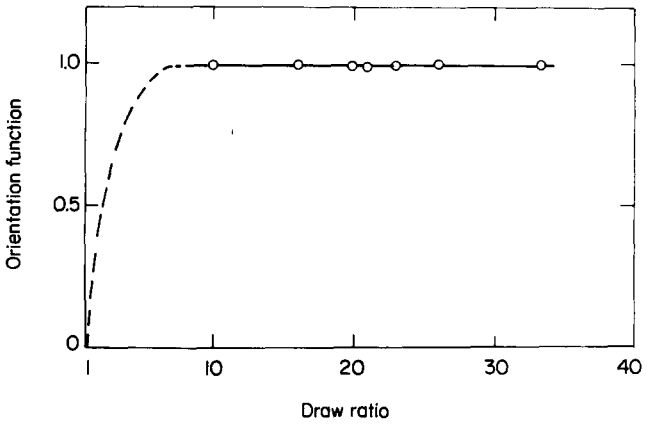

Figure 11 Orientation function vs. draw ratio for POM tubes

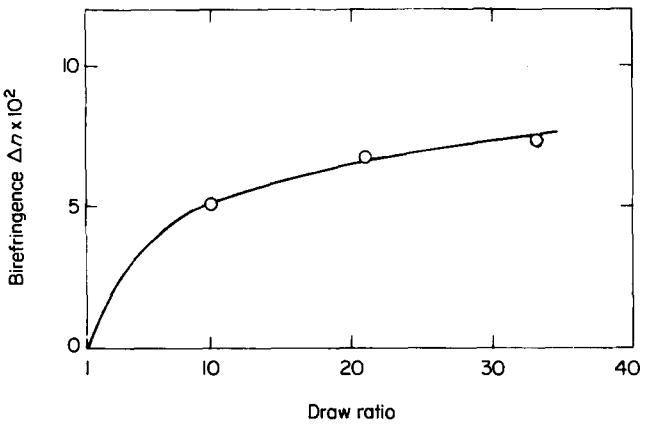

Figure 12 Birefringence vs. draw ratio for POM tubes

cross-section of drawn POM tubes. The birefringence increases with draw ratio. This behaviour is similar to that obtained by the hydrostatic extrusion[12]. The birefringence depends on the orientation of the crystalline and noncrystalline regions. Since crystalline orientation is almost constant (*Figure 11*), the increase in the birefringence at draw ratios over 10 is due to the increase in the amorphous orientation.

Non-uniformity in a radial direction

Figure 13 shows the optical micrographs of the cross-sections of drawn POM tubes (draw ratios of 10, 21 and 33). Nonuniformity of structure can be seen in the radial direction. *Figure 14* shows the scanning electron micrograph of the longitudinal sections drawn POM tubes (draw ratios of 10, 21 and 33). They show a fibrillar structure orienting along the draw direction. Nonuniformity of structure in the radial direction could not be observed in the scanning electron micrographs.

Figure 15 shows the sonic modulus in the inside and the outside parts of the drawn tubes. The sonic modulus of the inside part is the same as that of the outside at draw ratios of 10 and 21. But the sonic modulus of the inside part is larger than that of the outside at draw ratio of 33. *Figure 16* shows the melting temperature and the heat of fusion of the inside and outside parts of the drawn tubes. The melting temperature is the same at each draw ratio. The heat of fusion is the same at draw ratios of 10 and 21. But the heat of fusion of the inside part is larger than that for the outside at a draw ratio of 33. The difference in the heat of fusion is consistent with that of the sonic modulus. The crystal orientation function in the inside and the outside parts is the same at draw ratios over 10. *Figure 17* shows the variation of birefrigence in the radial direction. The

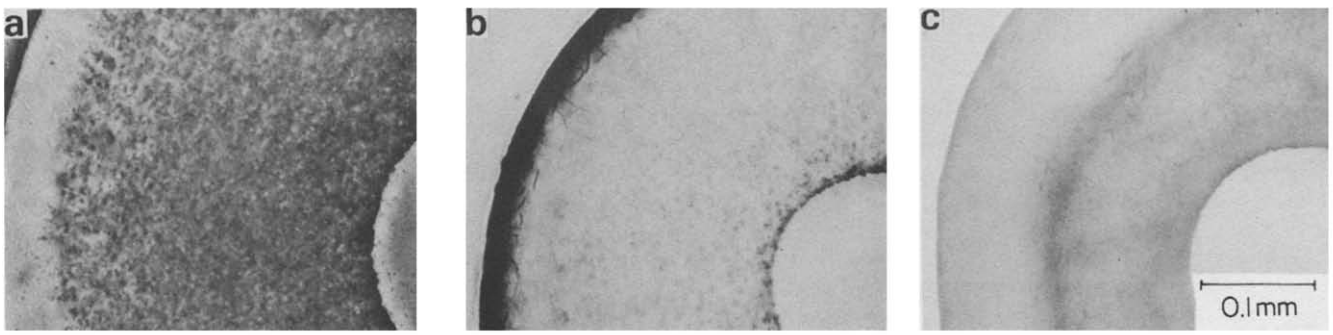

Figure 13 Optical micrographs of the cross section of POM tubes. Thickness *ca.* 0.2 mm

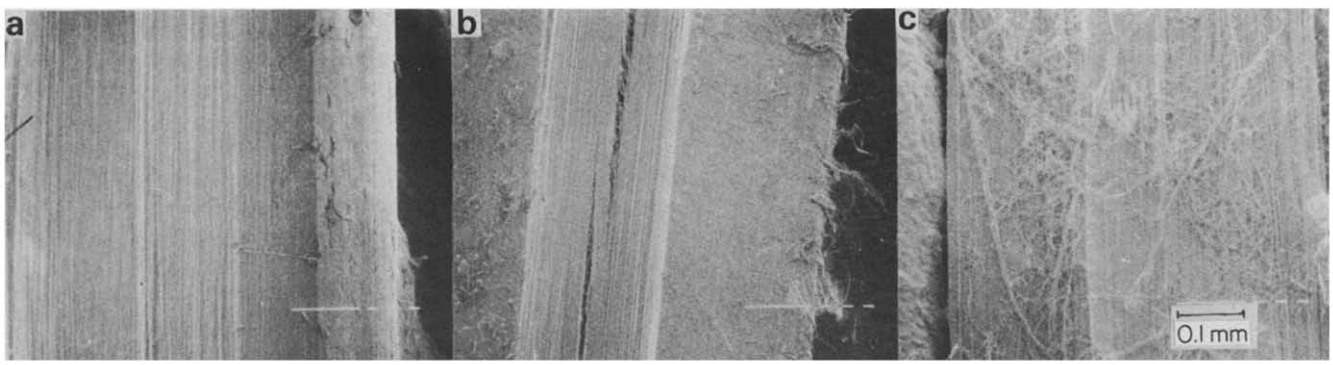

Figure 14 Scanning electron micrographs of the longitudinal section of POM tubes; draw ratios: (a) 10, (b) 21; (c) 33

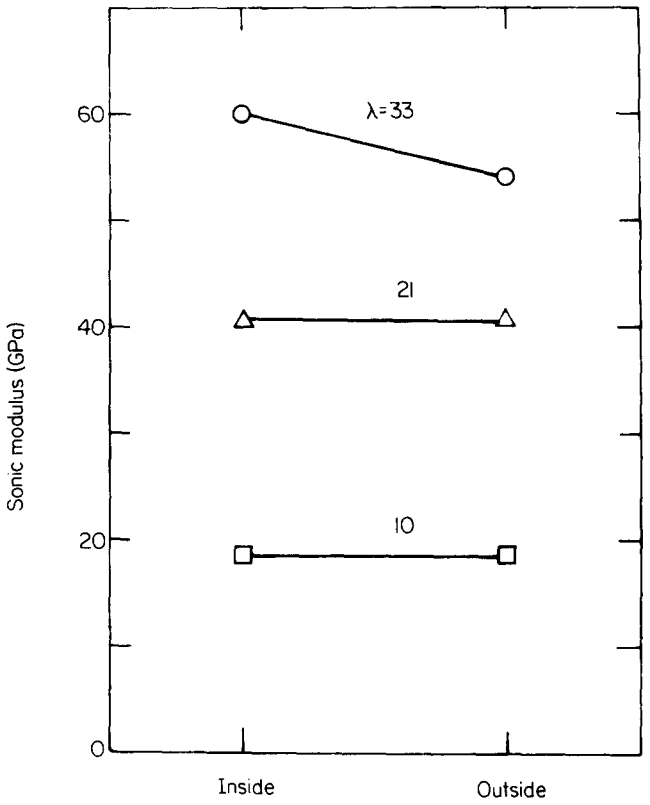

Figure 15 Nonuniformity of sonic modulus in a radical direction for POM tubes

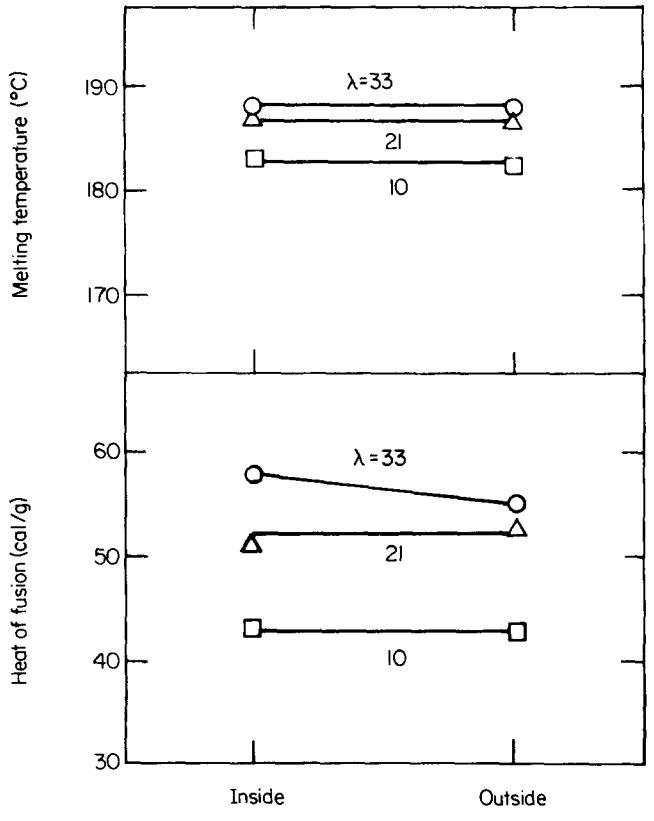

Figure 16 Non-uniformity of melting temperature and heat of fusion in a radical direction for POM tubes

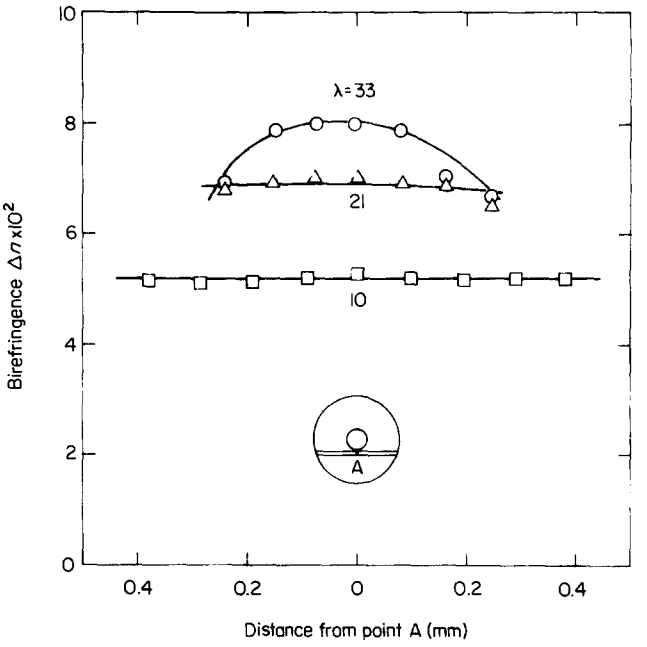

Figure 17 Variation of birefringence over the cross-section for POM tubes; draw ratios: (a) 10; (b) 21; (c) 33

birefringence is almost the same over the cross-section at draw ratios of 10 and 21. But the birefringence of the inside part is higher than that of the outside at a draw ratio of 33 in the same manner as the sonic modulus and the heat of fusion.

Nonuniformity in the properties cannot be seen in the radial direction at draw ratio of 10 and 21. But the inside part is more highly oriented than the outside at a draw ratio of 33. One reason for the occurrence of such nonuniformity is thought to be that the outside part was heated excessively because the ambient temperature was too high in the drawing process.

CONCLUSION

Ultra-high modulus and ultra-high strength POM tube can be produced by microwave heating and drawing. The highest Young's modulus was 58 GPa at room temperature at a draw ratio of 33 and the maximum tensile strength was 1.7 GPa at a draw ratio of 26. Nonuniformity of the properties in the radial direction was not observed up to a draw ratio of 21. But, at a draw ratio of 33, nonuniformity of Young's modulus was observed and compared with the nonuniformity of the heat of fusion and birefringence.

ACKNOWLEDGEMENT

The authors wish to thank K. Matsuyama, T. Kimura and N. Inagaki for their continuing guidance and encouragement. Thanks are also due to F. Yamamoto with whom they have had many useful discussions. They also would like to express their appreciation to Y. Takeuchi for the birefringence measurements.

REFERENCES

1 Ciferri, A. and Ward, I. M. 'Ultra-High Modulus Polymers', Applied Science, London, 1979

2 Sugeta, H. and Miyazawa, T. *Polym. J.* 1970, **1**, 226
3 Asahina, M. and Enomoto, S. *J. Polym. Sci.* 1962, **59**, 101
4 Piseri, L. and Zerbi, G. *J. Chem. Phys.* 1968, **48**, 3561
5 Sakurada, I., Nukushina, Y. and Ito, T. *J. Polym. Sci.* 1962, **57**, 651
6 Brew, B., Clements, J., Davies, G. R., Jakeways, R. and Ward, I. M. *J. Polym. Sci. Polym. Phys. Edn.* 1979, **17**, 351
7 Iguchi, M., Suehiro, T., Watanabe, Y., Nishi, Y. and Uryu, M. *J. Mater. Sci.* 1982, **17**, 1632
8 Takeuchi, Y., Yamamoto, F. and Nakagawa, K. *J. Polym. Sci. Polym. Lett. Edn.* 1984, **22**, 159
9 Rabolt, J. F. and Francoi, B. *J. Polym. Sci. Polym. Lett. Edn.* 1977, **15**, 121
10 Clark, E. S. and Scott, L. S. *Polym. Eng. Sci.* 1974, **14**, 682
11 Brew, B. and Ward, I. M. *Polymer* 1978, **19**, 1338
12 Coates, P. D. and Ward, I. M. *J. Polym. Sci. Polym. Phys. Edn.* 1978, **16**, 2031
13 Hope, P. S., Richardson, A. and Ward, I. M. *J. Appl. Polym. Sci.* 1981, **26**, 2879
14 Nakagawa, K., Maeda, O. and Yamakawa, S. *J. Polym. Sci. Polym. Lett. Edn.* 1983, **21**, 933
15 Nakagawa, K., Konaka, T. and Yamakawa, S. *Polymer* 1985, **26**, in press
16 Moseley, W. W. Jr. *J. Appl. Polym. Sci.* 1960, **3**, 266
17 Alexander, L. E. 'X-ray Diffraction Methods in Polymer Science', John Wiley, New York, 1969
18 Dunmbleton, J. H., Buchanan, D. R. and Bocules, B. B. *J. Appl. Polym. Sci.* 1968, **12**, 2067
19 McCrum, N. G., Read, B. F. and Williams, G. 'Anelastic and Dielectric Effects in Polymeric Solids', John Wiley and Sons, London, 1967, p. 540
20 Jarecki, L. and Meier, D. J. *J. Polym. Sci. Polym. Phys. Edn.* 1979, **17**, 1611
21 Iguchi, M. *Makromol. Chem.* 1976, **177**, 549